Characteristic analysis on morphological evolution of suspended particles in water during dynamic flocculation process

Jun Nan*, Weipeng He

*Skate Key Laboratory of Urban Water Resource and Environment, School of Municipal and Environmental Engineering, Harbin Institute of Technology, Harbin 150090, PR China
Tel. +86 451 86084169; Fax: +86 451 86283001; email: nanjun_hit@163.com*

ABSTRACT

The evolution of floc morphology during constant-speed and variable-speed flocculation was examined to understand floc growth mechanisms. Flocculation-test results were reported in terms of floc average size and fractal dimension, derived from *in situ* optical sampling and image analysis. The morphological evolution was also described using a fractal growth model, which defined flocculation as the combined processes of aggregation and restructuring. During constant-speed flocculation, aggregation rate increased with increasing shear, but breakage became significant. Also, a decrease was observed after reaching the peak of size, possibly due to floc settling in low shear and the irreversibility of breakage in high shear. The development of floc morphology in variable-speed flocculation indicated that the surface nature of initial flocs was critical to form larger final flocs, because aggregates with irregular shape had more connection spots than those with smooth surface, thus producing a higher aggregation rate for further growth. As expected, longer duration of slow stirring at the first stage produced lower flocculation efficiency because of the change of surface properties by restructuring. Additionally, steady state was attained faster for floc structure than for size at the same shear during whatever flocculation, possibly due to the self-similarity of fractal aggregates.

Keywords: Flocculation; Fractal dimension; Breakage; Image analysis

1. Introduction

In water treatment, it is critical to ensure maximum removal of suspended particles, as they can lower water quality and damage the supply and distribution systems. Particle removal from a suspension by sedimentation following flocculation is widely applied at water treatment works (WTWs) [1–3]. During the process of flocculation, small particles destabilized by chemical coagulant/flocculant are encouraged to contact with each other, forming highly porous and irregularly shaped aggregates, known as flocs [4]. Maximizing the size of the final flocs is of great importance, because smaller particles generally settle more slowly than larger particles of similar density [5]. The evolution of floc size during flocculation is accomplished by the change of floc structure [6]. Apparently, floc morphology (here, i.e. size and structure) may directly affect the removal efficiency of suspended particles during particle separation.

Most previous studies have demonstrated that the development of floc morphology is governed by the combined processes of aggregation, breakage, and reformation [2,7–9]. Initially, particle aggregation is

---

*Corresponding author.

dominant. During this time period, suspended particles aggregate rapidly due to a high rate of interparticle collisions. As flocculation continues, flocs become larger and may be more susceptible to breakage by fluid shear. After a certain time, aggregation and breakage balance each other, resulting in a steady-state floc size distribution. Also, floc structure may be made more compact [10]. This suggests that if properly controlled, flocculation can be used to produce aggregates with desired morphology [8]. Therefore, it is desirable to have a good quantitative understanding of the growth mechanisms which control the flocculation process.

Floc strength is another particularly important operational parameter and plays a significant role in the effectiveness of WTWs [11]. Unfortunately, water treatment processes are often non-ideal with regions of high shear being prevalent [10], which may introduce breakage of flocs. Therefore, flocs must resist these stresses to prevent being broken into smaller particles or clusters. It is generally accepted that floc strength is directly related to floc structure, and thus highly dependent on the floc formation process [12–14]. Increased floc compaction may increase floc strength due to an increase in the number of bonds holding the aggregate together [11]. Irregular aggregate structures have usually been quantified by utilizing the fractal concepts, which essentially recognize that aggregates possess self-similar structures [8,9,15].

Factors affecting flocculation process include coagulant type and dosage, particle concentration, solution pH, mixing intensity, and duration [16]. An open issue refers to the effect of shear history on steady-state properties of flocs [8]. When a precipitated/polymeric flocculant is used, floc morphology is found to be strongly dependent upon how the shear is varied before reaching the steady state [17]. Serra et al. [6], Soos et al. [8], and Selomulya et al. [18] found that the larger the shear the smaller the average/median size under steady-state conditions. On the contrary, Colomer et al. [16] investigated particle aggregation and breakage in low-shear flow by monitoring the final aggregate size distribution, and reported that average size increases with increasing shear. A recent study was conducted by Serra et al. [2] to examine particle flocculation in three different devices (paddle mixer, oscillating grid, and Couette), showing that each device has a shear rate for which there is a transition from aggregation-dominated conditions to breakage dominated conditions. All these findings indicated that it is essential to evaluate the behavior and efficiency of flocculation under different shear conditions. Also, the mechanisms involved should receive enough attention.

In the present study, a series of flocculation tests were carried out to investigate the evolution of floc morphology during dynamic flocculation process. Results were reported in terms of floc average size (d_p) and boundary fractal dimension (D_{pf}), derived from a non-intrusive optical sampling and digital image analysis technique. In addition, a fractal model of floc growth, which defined flocculation as the result of the combined processes of aggregation and restructuring, was proposed to explore the growth mechanisms of flocs. We were particularly interested in how an increase in the shear affected flocculation behavior and efficiency. This topic has important implications for particle formation in the engineering aspects.

2. Materials and methods

2.1. Suspension

Kaolin clay (Tianjin, China) suspension was used as testing water sample. The stock suspension was prepared similar to that of Yukselen and Gregory [19]. The particles had an average size of about 3 μm (Fig. 1), determined by a particle counter (2200PCX, HACH, USA).

For flocculation tests, the stock solution was diluted in the tap water of Harbin, China, giving a final clay concentration of 100 mg/L. Harbin tap water has medium total hardness (ca. 160 mg/L as $CaCO_3$) and alkalinity (ca. 115 mg/L as $CaCO_3$) and a pH of around 7.8. To avoid the disturbance of divalent metal ions such as Ca^{2+} and Mg^{2+} in tap water, a small amount of humic acid (Shanghai, China) was added into the testing sample [1]. The final suspension containing 100 mg/L kaolin and 2 mg/L humic acid had a turbidity of about 100 NTU, determined by an online turbidimeter (700AQ, WTW, Germany). All the
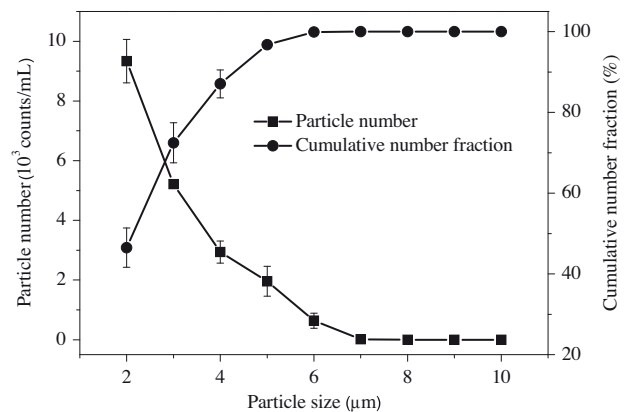

Fig. 1. Particle size distribution in testing water samples before coagulant addition. The size and number of particles were determined by a PCX 2200 Particle Counter (HACH, USA). Error bars represent the standard deviation for each point.

tests were conducted at room temperature $(22 \pm 1°C)$ and replicated 2–3 times.

2.2. Coagulant

Polyaluminum chloride (PACl) was selected as the coagulant to form colloid aggregates. Stock PACl solutions of 1% w/w were prepared by dissolving the reagent in deionized water (5 g dissolved in deionized water to 500 mL) and, for the flocculation tests, directly pipetted in the testing water without further dilution.

2.3. Characteristics of the stirred tank

The flocculating reactor used in this study was a rectangular stirred tank (homemade) with a bottom length $D = 280$ mm and a liquid height $H = 230$ mm, and filled with 18 L of testing water sample (see Section 2.1) as working fluid. For agitation, a R1342-type impeller (IKA, Germany) with a diameter $d = 50$ mm was used and the center of the impeller was positioned at $C = H/3$ from the tank bottom. This mixing system was successfully used in some of our previous studies, e.g. in [3].

2.4. Experimental procedure

Optimal PACl dosage was first determined by performing a series of flocculation tests with incremental increases in the coagulant dose (between 1 and 10 mg/L as Al). For each test, after a certain amount of PACl coagulant dosed in the reactor, the testing suspension (100 mg/L kaolin and 2 mg/L humic acid in Harbin tap water) was mixed rapidly at 400 rpm for 30 s, followed by a slow stirring phase at 100 rpm for 20 min. Then the turbidity of supernatant (at 5 cm below the liquid surface) was measured, after a 20-min sedimentation (without mixing), by an online turbidimeter (700AQ, WTW, Germany). The amount of coagulant giving the minimum turbidity is the optimal dosage [20], which was then used for all other tests in this study.

For dynamic tests, after allowing 1 min for steady-state turbidity (measured by online turbidimeter) to be established, PACl solution was dosed and the suspension was rapidly mixed at 400 rpm for 30 s, followed by a slow stirring phase for flocculation. In order to evaluate the effect of shear history on floc morphology, two modes of flocculation processes were performed. The first one was called constant-speed flocculation, where destabilized particles aggregate at a constant slow stirring speed. For this mode

of flocculation, the stirring speed (N) was reduced to 50, 70, 110, 120, and 140 rpm, respectively, for 39 min following the rapid mixing. In the second mode of flocculation, flocs were formed under tapered-shear conditions, called variable-speed flocculation, which was commonly used to minimize floc breakage but maximize particle collisions at WTWs [10,21]. In this study, the process of variable-speed flocculation was divided into three stages to investigate the evolution of floc morphology with different time combinations (TC). The slow stirring speed for each stage was 140, 70, and 50 rpm, and the corresponding time groups used here were: (1) TC I, 5 + 9 + 13 min; (2) TC II, 9 + 9 + 9 min; and (3) TC III, 13 + 9 + 5 min. Taking "TC I" for example, flocculation tests were carried out as follows: after the rapid mixing, the suspension was mixed at 140 rpm for 5 min, followed by a further slow stirring at 70 rpm for 9 min and 50 rpm for 13 min, successively. The flocculation processes of TC II and TC III were similar to that of TC I.

In all flocculation tests, the Reynolds number for the impeller $(Re = Nd^2/v$, where v is the kinematic viscosity of the water) was larger than 1,000, corresponding to turbulent mixing.

2.5. In-situ recognition for floc morphology

A modified version of the standard flocculation-test procedure was used in this work (Fig. 2). From the moment of coagulant addition, a non-intrusive optical sampling technique was used to obtain digital images of particles (Fig. 3), which were then analyzed to develop floc size and structural properties, and calculations of the fractal dimension. The basic procedures were adapted from the work of Chakraborti et al. [22], who studied aggregate characteristics produced after mixing suspensions with different coagulant doses. A major advantage of their method is that it requires no sample handling, so there is no concern for disturbing the floc characteristics during measurements. A similar measurement technique was used by Xiao et al. [13] to investigate the flocculation dynamics for different coagulants in different model waters.

In the present work, the *in situ* recognition system consisted of an automated stroboscopic lamp to illuminate suspended particles in the tank, a high-speed digital charged-coupled device (CCD) video camera (GmbH, Germany) with a resolution of 992(horizontal) × 510(vertical) pixels to capture particle images and a process control and image processing software package (FMans 10, China) to determine floc geometrical parameters (Fig. 2). The camera was placed on the opposite side of the tank from the lamp, so that
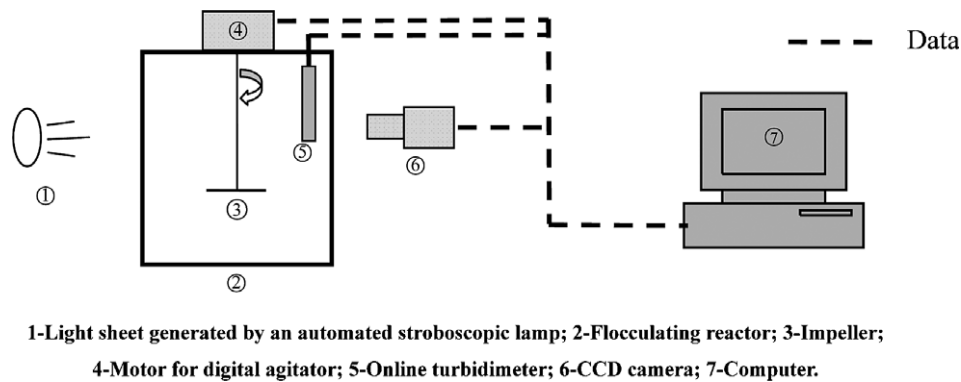
1-Light sheet generated by an automated stroboscopic lamp; 2-Flocculating reactor; 3-Impeller;
4-Motor for digital agitator; 5-Online turbidimeter; 6-CCD camera; 7-Computer.

Fig. 2. Schematic of the *in situ* recognition technique for floc morphology.
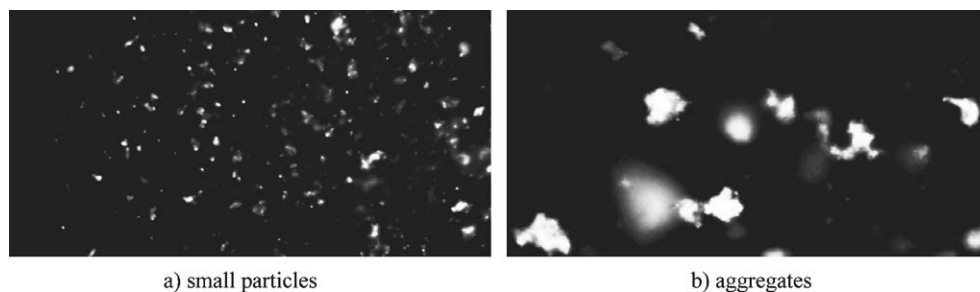

a) small particles   b) aggregates

Fig. 3. Examples of floc images captured *in situ* during a typical flocculation process.

backlit shadows of particles were produced. A personal computer served to control the camera and provided storage for particle images.

Images were taken to examine aggregate geometry and size distributions at different moments (here, every second) during each test. The images were then analyzed to track changes in aggregate morphology for a given experiment, as well as differences between experiments resulting from varying mixing speed (N). The analyses were reported in terms of the fractal dimension and associated floc average size (see Section 2.6). Before processing a particular image, image thresholding was applied, where pixels were classified into two categories, either background or particle. This step effectively filtered out random noise, as well as particles that were not well focused. Based on calibration, the monitoring system had a resolution of around 5.7 μm for particle tracking and imaging in the present flocculation study. More than 10 consecutive images within a minute were analyzed to produce floc morphological parameters.

2.6. Floc size and fractal dimension by image analysis

Flocs generated during flocculation have been shown to be fractal, implying that they are self-similar and scale invariant [9,10,23]. For a floc of irregular shape, its size, d_p, can be calculated in terms of the equivalent diameter by

$$d_p = (4A/\pi)^{1/2} \tag{1}$$

where A is the projected area of the floc. Then the average size of flocs in more than 10 images within a minute was used to reflect the size distribution at the corresponding moment.

In addition to floc average size, a boundary fractal dimension was used to characterize the fractal properties of flocs. For a two-dimensional projected particle image, the fractal dimension, D_{pf}, defines how the projected area of the particles scales up with the length of the perimeter [17,24] according to

$$A \propto P^{2/D_{pf}} \tag{2}$$

where P is the perimeter of an aggregate. Since D_{pf} depicts the surface morphology of the aggregate in two-dimensional projection, its value ranges from $D_{pf} = 1$ for the projected area of a sphere (a circle), to $D_{pf} = 2$ for a line (e.g. a chain of particles) [15]. Moreover, the mass fractal dimension, D_f, is also a measure of floc structure and varies from 1 for a line of

particles to 3 for a sphere [18], but there is no straight-forward relationship between D_f and D_{pf} [25]. In this study, flocs in more than 10 images within a minute were used to calculate the value of D_{pf} at the corresponding moment.

3. Results and discussion

3.1. Coagulant optimization

Initial flocculation tests were conducted to determine the optimal flocculant dosage, as described earlier. Turbidity removal rate reached a peak value of about 90% at the PACl dosage of 2.2 mg/L as Al, which was selected as the optimal dosage and then used for all other flocculation tests in this study.

3.2. Evolution of floc size and structure during constant-speed flocculation

The *in situ* recognition technique for floc morphology (Fig. 2) is shown to be a powerful tool for performing real-time, *in situ* particle imaging acquisition to determine floc size distribution during flocculation, expressed as temporal changes in floc average size (d_p) at different slow stirring speeds (Fig. 4a). The high-quality floc images captured (Fig. 3) also allow detailed analysis of floc structural features, reported in terms of the boundary fractal dimension (D_{pf}) of aggregates (Fig. 4b). According to Eq. (2), the D_{pf} could be approximated from the slope of log–log regression of a series of projected areas vs. perimeters of the particles. In general, a higher D_{pf} normally indicates a more irregular and/or elongated shape and a rougher surface for the particles, whereas a lower D_{pf} suggests a more spherical shape and a smoother surface of the particles [13,26,27]. The D_{pf} at steady state ranged from 1.13 to 1.24 (Fig. 4b). This was similar to the range reported for the kaolin-HA flocs after 30 min of slow flocculation by Xiao et al. [13], but somewhat lower than the values (from 1.10 to 1.40) reported for the aggregates of polystyrene spheres [27].

The rate of floc growth (R_{floc}) may be considered as the difference between the rate of aggregation and the rate of floc breakage (R_{br}) [11]:

$$R_{floc} = \alpha R_{col} - R_{br} \tag{3}$$

where R_{col} is the rate of particle collision, α is the fraction of collisions which result in attachment ($0 < \alpha < 1$), and αR_{col} is used to represent the rate of aggregation. It is apparent that when the two terms on the right-hand side of Eq. (3) are equal, the net rate of floc
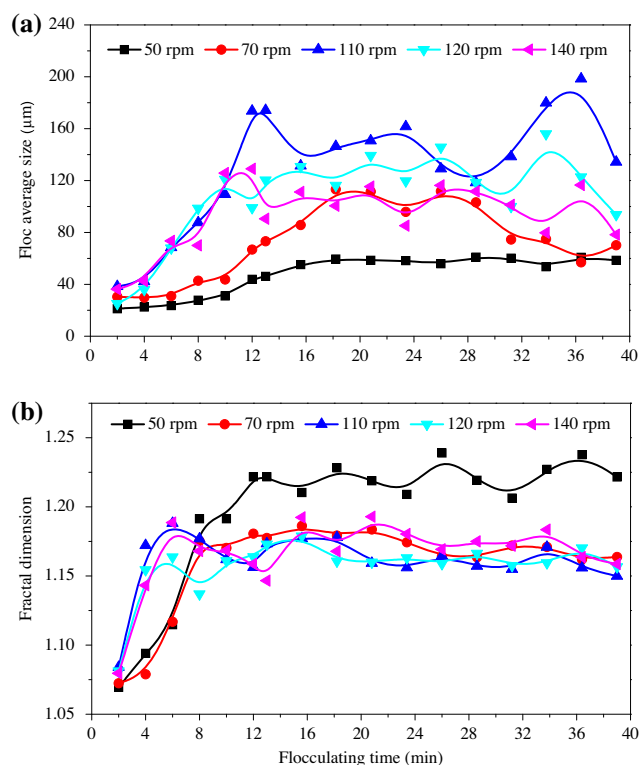

Fig. 4. Variation in (a) floc average size and (b) boundary fractal dimension with flocculation time under different slow stirring speeds. (PACl dosage, 2.2 mg/L as Al; rapid stirring, 400 rpm for 30 s; slow stirring time, 39 min.)

growth is zero and the floc size attains a limiting value. This is of great importance in understanding the evolution of floc morphology under different shear conditions. At the beginning of flocculation, a rapid increase in d_p and D_{pf} was observed for each speed of slow stirring (Fig. 4), indicating that floc aggregation seemed to be dominant and breakage (being probably occurring) might be relatively unimportant to the development of floc size and structure during this time period. In this case, the growth of flocs was only determined by the collision efficiency, i.e., $R_{floc} \approx \alpha R_{col}$. As the shear increased, the circulation time ($t_c = V/(N_q N d^3)$, where V is the volume of water, and N_q is the dimensionless impeller pumping capacity) became shorter, indicating that the flocs were exposed to the high-shear impeller zone more frequently, resulting in an increased rate of particle collision [7,28]. Therefore, the growth in aggregate size became faster with increasing speed of slow stirring (Fig. 4a). Also, a similar phenomenon was observed for the floc structure (Fig. 4b).

However, as the particle (floc) size increased for a constant shear, αR_{col} decreased [29], and breakage became significant ($R_{br} \neq 0$) [30]. When $R_{floc} = 0$, no
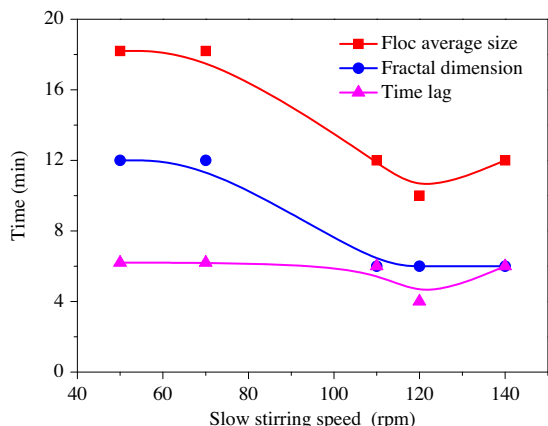
Fig. 5. Flocculation time (t_s) required to reach steady state for floc size and fractal dimension under different slow stirring speeds. The time lag at the same speeds is also given here. (PACl dosage, 2.2 mg/L as Al; rapid stirring, 400 rpm for 30 s; slow stirring time, 39 min.)

further growth would occur, and a steady state was reached (Fig. 4). This was usually assumed to represent a dynamic balance between shear-induced aggregation and breakage [7,8,18]. As expected, an increase in the shear caused a reduction in the flocculation time (t_s) that was required to reach steady state for d_p and D_{pf}, but steady state was attained faster for D_{pf} than for d_p at the same slow stirring speeds (Fig. 5), possibly due to the self-similarity of fractal aggregates [9,25].

The effect of shear on floc morphology at steady state during constant-speed flocculation was further investigated (Fig. 6). When the applied shear
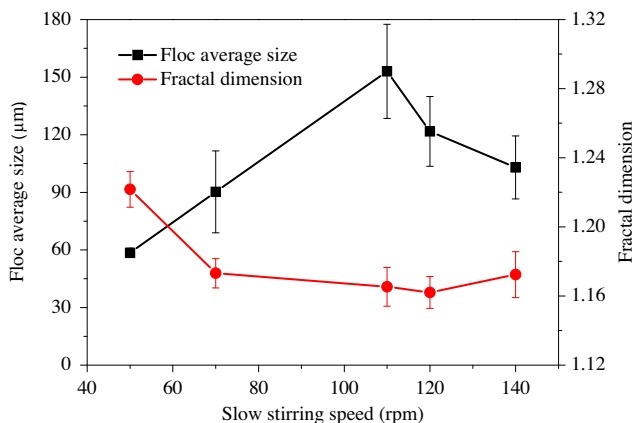
Fig. 6. Floc average size and boundary fractal dimension at steady state under different slow stirring speeds. Error bars represent the fluctuation degree, characterized by the standard deviation, of the two parameters at steady state for each stirring speed. (PACl dosage, 2.2 mg/L as Al; rapid stirring, 400 rpm for 30 s; slow stirring time, 39 min.)

increased from 50 to 110 rpm, the floc average size (d_p) increased from 58 ± 3 to 153 ± 24 μm, and the boundary fractal dimension (D_{pf}) decreased from 1.21 ± 0.01 to 1.16 ± 0.01, indicating the formation of larger aggregates with a more spherical shape and smoother surface. In particular, at 110 rpm, the d_p reached the maximum value, and the D_{pf} reached the minimum value, suggesting that the largest flocs with most compact structure were produced. For the higher speed values of slow stirring (e.g. 120 and 140 rpm), the d_p began to decrease but the D_{pf} slightly varied around 1.16 (Fig. 6), possibly due to the occurrence of breakage. The overall variation trend floc size was similar to that of Serra et al. [2], who defined three shear ranges, i.e. low shear, where the aggregation dominated over breakage and aggregate growth rate increased in proportion to the shear; intermediate shear, where flocculation rates were maximized and breakage minimized; and large shear, where breakage dominated aggregation, although sufficient collisions occurred to encourage the rate of aggregation.

An interesting observation from Fig. 4a was that the flocs grown at high shear (notably at 70, 110, and 140 rpm) exhibited some decrease after reaching the peak of size. For example, at 70 rpm, the flocs seemed to reach their maximum size of 113 μm early in the process before reducing to their final equilibrium size of about 70 μm. A similar phenomenon of a decrease to a steady-state size was observed by other workers, such as Wang et al. [10] and Selomulya et al. [18]. This behavior was possibly attributed to the nature of flow generated by the employed impeller under various slow stirring speeds (N). In the aggregation-dominated range ($N < 110$ rpm), the frequency of circulation through the high-shear impeller zone was relatively low, resulting in the slow formation of flocs with open and porous structure (Fig. 4b), which had large pores. These pores likely permitted great quantities of flow through them, thus attaining large settling velocities [23]. Therefore, floc size decreased in this shear range, mainly due to floc settling at steady state. As discussed above, the higher the shear, the shorter the circulation time (t_c). At 110 rpm or above, the shorter t_c could produce more sufficient collisions to make larger aggregates, but further exposure to the impeller zone would introduce floc breakage and restructuring, leading to a lower final equilibrium size due to the irreversibility of PACl-floc breakage [1].

3.3. Fractal model of floc growth

In order to improve the understanding of aggregate structure and its growth process, a number of fractal aggregation models, including the diffusion-

limited aggregation (DLA) model and its several variations (reaction-limited, cluster-particle, cluster–cluster, etc.), have been established [24,31,32]. These models usually consider aggregation as an irreversible process neglecting breakage and restructuring. This is a critical limitation, when compared with naturally occurring processes, where a restructuring of primary particles occurs within an aggregate due to breakage and reformation [9]. As suggested by Becker et al. [33], the restructuring behavior of colloidal aggregates with different sizes was quite different in shear flows (Table 1).
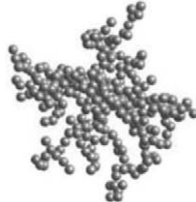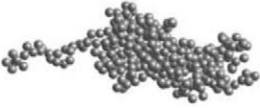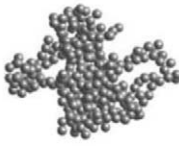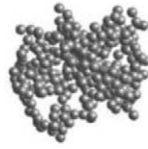
Based on the results shown in Figs. 4 and 6, a fractal model of floc growth was proposed to describe the dynamic process of flocculation. In this model, flocculation was defined as the result of the combined processes of aggregation, breakage, and restructuring (Fig. 7). Initially, destabilized particles are transferred into contact with each other by the applied shear, producing small clusters in the DLA limit. Further aggregation mainly occurs among those small clusters resembling the cluster–cluster aggregation (CCA) model, producing larger flocs with more highly branched structure. As flocculation continues, these existing aggregates become more susceptible to breakage and would break up at their weakest points, followed by reformation. After a certain time, breakage and reformation can lead to stronger and more compact flocs (Fig. 7), with an associated lower boundary fractal dimension (D_{pf}). Similar results have been reported by Xiao et al. [13], and Stone and Krishnappan [34], for example.

Now let us focus on the evolution of floc morphology during constant-speed flocculation (Figs. 4 and 6). At low shear ($N < 110$ rpm), it seemed that little breakage occurred and particles/flocs aggregated in the DLA/CCA limit for the overall process. In this case, the growth of flocs only depended on the collision efficiency resulting from the effective shear, but further growth was limited by low particle collision rates of larger particles with other particles. At 50 rpm, aggregation rate was minimized due to the lowest particle collision, producing the smallest flocs with the loosest structure (Fig. 6). It was possible that these flocs might rotate like Aggregate I (Table 1) without any structural change in shear flow. Therefore, at steady state no significant fluctuation was observed for floc size and structure (Fig. 4). As expected, when the shear increased to 70 rpm, the formed flocs were larger (Fig. 6) due to increased particle collisions. Some of these flocs with intermediate size appeared to undergo a restructuring process resembling Aggregate II (Table 1), starting with an initial stretching phase. This behavior may be another reason for the production of larger flocs with more compact structure.

Table 1
Schematic of the structural evolution models of aggregates in shear flows. These models were proposed by Becker et al. [33], who investigated the restructuring behavior of colloidal aggregates in shear flows. Aggregate I, composed of 55 primary particles, rotates like a rigid body without structural change; Aggregate II, composed of 305 primary particles, undergoes restructuring, starting with an initial stretching phase, followed by an aggregate compaction; Aggregate III, composed of 1,000 primary particles, breaks up under shear stress. Please refer to [33] for more details

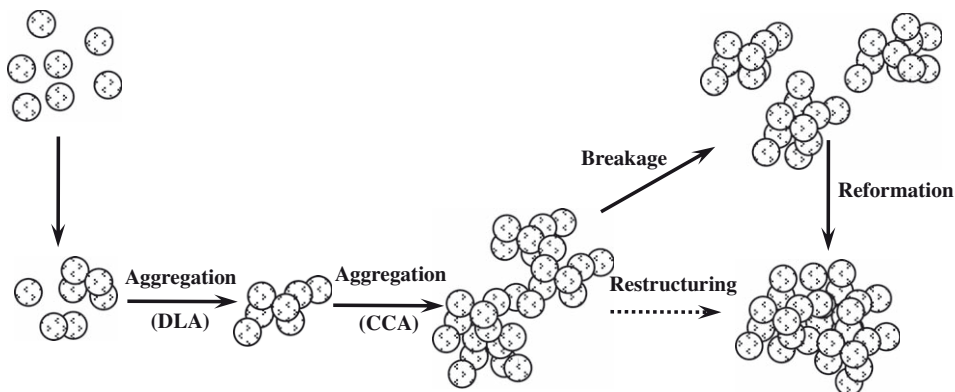| Aggregate	Temporal evolution of aggregate structure (from left to right)
I	
II	
III	

Fig. 7. Schematic of floc growth during flocculation. Initially, destabilized particles form small clusters resembling the DLA model. These clusters further collide to produce larger aggregates with highly branched structure in the CCA limit. As flocculation continues, there is a restructuring of primary particles within an aggregate due to breakage and reformation that occurs in response to local shear, leading eventually to stronger and more compact aggregate structure.

When the shear varied from 110 to 140 rpm (Figs. 4 and 6), floc breakage seemed to be significant. Some of the CCA aggregates (Fig. 7) began to break up like Aggregate III (Table 1). After breakage, the elongated flocs broke up into smaller pieces that were more close to spherical objects than the original flocs [13]. In addition, during the process of floc breakage and reformation, the surface of large flocs might be destroyed, disclosing some inner pores hidden in these aggregates [10], and thus small particles or clusters had more opportunity to be incorporated into these larger flocs. This behavior would not only improve floc structure but also reduce the number of small particles.

3.4. Evolution of floc size and structure during variable-speed flocculation

Floc strength is greatly related to the floc growth process, as mentioned above. The evolution of floc morphology during constant-speed flocculation (Fig. 4) indicated that the rate of floc aggregation increased with increasing the shear, but breakage became more significant at higher shear. To encourage particle aggregation and prevent floc breakage, flocculators at WTWs are generally designed by using gradual reduction of the applied shear, with the goal of the formation of large flocs with excellent settling performance [11,13].

This section mainly focused on the effect of flocculation TC on the development of floc morphology, derived from the *in situ* recognition technique (Fig. 2). In this study, the process of variable-speed flocculation was divided into three stages, and the slow stirring speed (N) for each stage was 140, 70, and 50 rpm. Many corresponding time groups have been evaluated, but only three of them (i.e. TC I–III) were selected and given here (Fig. 8), to illustrate a significant aspect of the results.

Fig. 8a shows temporal changes in floc average size (d_p) and boundary fractal dimension (D_{pf}) during variable-speed flocculation of TC I (5 + 9 + 13 min). When the slow stirring was set at 140 rpm for 5 min, a rapid increase in d_p and D_{pf} could be observed. This was because floc aggregation in the DLA/CCA limit dominated over breakage and the applied shear of 140 rpm produced a high rate of particle collision. When the shear was reduced to 70 rpm, the d_p increased from 65 to 93 μm in the first 3 min, and then decreased slightly to a final steady-state size of about 70 μm as a result of shear-induced restructuring of CCA aggregates [33]. Further reduction of the shear to 50 rpm resulted in a similar variation trend of d_p with that in the second stage (N = 70 rpm), but the steady state d_p seemed to be slightly larger. This was possibly due to the fact that chemical bonds may be broken during floc disruption [1] and the subsequent reformation rate increases with decreasing fragmentation shear [26]. Furthermore, the D_{pf} reached steady state at the end of the first stage and then fluctuated greatly at around 1.20 in the last two stages. Interestingly, after about 21 min, the fluctuation of D_{pf} became insignificant (Fig. 8a), indicating the formation of more compact flocs with greater strength.

In the first stage of variable-speed flocculation of TC II (9 + 9 + 9 min), the d_p increased from 24 to 113 μm (Fig. 8b), indicating a rapid growth in floc size due to a frequent exposure of the particles to the high-shear impeller zone [7], whereas the D_{pf} increased rapidly to 1.20 in the first 5 min and then slightly changed. When the N was reduced from 140 to 70 rpm, both of d_p and D_{pf} greatly fluctuated as a result of the occurrence of more intense restructuring of CCA aggregates. At the third stage (N = 50 rpm), the existing flocs continued to restructure in the first 4 min (from 18 to 22 min), but
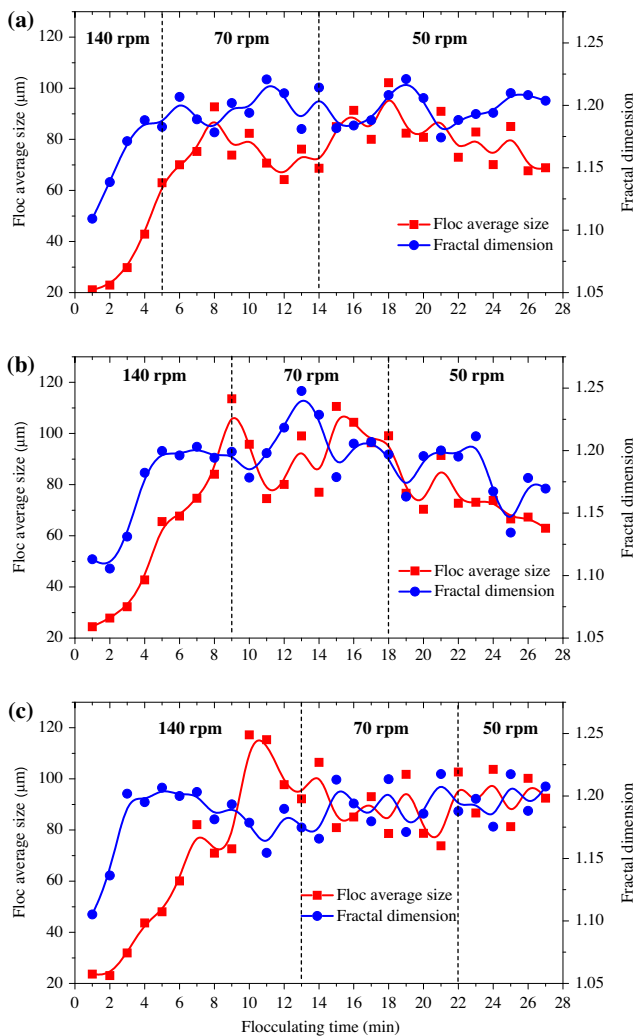
Fig. 8. Variation in floc average size and boundary fractal dimension with flocculation time during variable-speed flocculation. The testing suspension was rapidly mixed at 400 rpm for 30 s, followed by a slow stirring phase with three stages. The slow stirring speed for each stage was 140, 70, and 50 rpm, and the corresponding time groups used here were: (a) TC I, 5 + 9 + 13 min; (b) TC II, 9 + 9 + 9 min; and (c) TC III, 13 + 9 + 5 min. (PACl dosage, 2.2 mg/L as Al.)

further exposure of the particles to the shear produced a reduction in d_p and D_{pf} (Fig. 8b), possibly because some loose flocs began to settle at about 23 min.

Longer duration of slow stirring at 140 rpm decreased d_p and D_{pf} after about 9 min (Fig. 8c), suggesting that some elongated flocs might be broken up into small pieces, with a more spherical shape and smoother surface. The reconnection of these fragments seemed to be rather poor, and therefore the d_p and D_{pf} had no significant change in the last two stages. In addition, more scatter in d_p was observed in the second stage than in the third stage, and the same is

true of D_{pf} (Fig. 8c). This phenomenon possibly resulted from the higher shear applied in the second stage, which produced a more frequent exposure of the aggregates to the impeller zone and thus more intense restructuring of CCA aggregates.

The evolution of floc morphology during variable-speed flocculation of TC I, TC II, and TC III (Fig. 8c) indicated that the formation of final flocs seemed to be greatly related to the floc properties formed in the initial process of flocculation. This was consistent with the fractal model of floc growth (Fig. 7). As suggested by many investigators, such as Spicer and Pratsinis [26], Stone and Krishnappan [34], and Wang et al. [10], the surface nature of flocs is changed in the combined processes of breakage and reformation, which made existing flocs more compact (Table 1), thus significantly reducing connection spots inside the aggregates (Fig. 7). This may be another reason why changes in d_p and D_{pf} were not significant in the last two stages of variable-speed flocculation of TC III (Fig. 8), indicating that the surface nature of initial flocs (micro-flocs or small clusters) is of great importance in forming larger flocs at the late stage of flocculation.

4. Conclusions

The main conclusions of this study were listed as follows:

1. Temporal changes in floc morphology (here, i.e. size and structure), derived from the *in situ* recognition technique, clearly exhibited the continuous floc growth during constant-speed and variable-speed flocculation. The development of floc size and structure was also described using a fractal growth model, which defined flocculation as the result of the combined processes of aggregation, breakage, and reformation.

2. For constant-speed flocculation, the rate of floc aggregation increased with increasing shear, but breakage became more significant at higher shear.

3. There was a decrease after reaching the peak of size under the examined speeds of slow stirring (N) during constant-speed flocculation. At low shear ($N < 110$ rpm), the formed flocs, with open and porous structure, likely permitted great quantities of flow through them to attain large settle velocities, thus making some porous flocs settling in the late stage; and at high shear (110 rpm and above), where floc breakage became significant, the decreased final equilibrium size was possibly attributed to the irreversibility of PACl-floc breakage.

4. The process of variable-speed flocculation, where flocs were formed under tapered-shear conditions

to minimize floc breakage, was divided into three stages with slow stirring speed of 140, 70, and 50 rpm for each stage, to investigate the evolution of floc morphology with different TC. The surface nature of initial flocs (micro-flocs or small clusters) was found to be of great importance in forming larger flocs at the late stage of flocculation. This was possibly due to the fact that initial flocs with irregular shape had more connection spots inside the aggregates than those with smooth surface.

5. For variable-speed flocculation with longer duration of slow stirring at the first stage, some elongated flocs might be broken up into small pieces, producing lower flocculation efficiency because of the change of floc surface properties by restructuring.

6. Steady state was attained faster for floc structure than for size at the same shear during constant-speed flocculation, possibly due to the self-similarity of fractal aggregates. This finding was also true of variable-speed flocculation.

Acknowledgments

References

[1] M. Yukselen, J. Gregory, The reversibility of floc breakage, Int. J. Miner. Process. 73 (2004) 251–259.
[2] T. Serra, J. Colomer, B.E. Logan, Efficiency of different shear devices on flocculation, Water Res. 42 (2008) 1113–1121.
[3] J. Nan, W. He, X. Song, G. Li, Impact of dynamic distribution of floc particles on flocculation effect, J. Environ. Sci. 21 (2009) 1059–1065.
[4] J. Duan, J. Gregory, Coagulation by hydrolysing metal salts, Adv. Colloid Interface Sci. 100–102 (2003) 475–502.
[5] M. Boller, S. Blaser, Particles under stress, Water Sci. Technol. 37 (1998) 9–29.
[6] T. Serra, J. Colomer, X. Casamitjana, Aggregation and breakup of particles in a shear flow, J. Colloid Interf. Sci. 187 (1997) 466–473.
[7] P.T. Spicer, W. Keller, S.E. Pratsinis, The effect of impeller type on floc size and structure during shear-induced flocculation, J. Colloid Interf. Sci. 184 (1996) 112–122.
[8] M. Soos, A.S. Moussa, L. Ehrl, J. Sefcik, H. Wu, M. Morbidelli, Effect of shear rate on aggregate size and morphology investigated under turbulent conditions in stirred tank, J. Colloid Interf. Sci. 319 (2008) 577–589.
[9] R.K. Chakraborti, K.H. Gardner, J.F. Atkinson, J.E.V. Benschoten, Changes in fractal dimension during aggregation, Water Res. 37 (2003) 873–883.
[10] D. Wang, R. Wu, Y. Jiang, C.W.K. Chow, Characterization of floc structure and strength: Role of changing shear rates under various coagulation mechanisms, Colloids Surf. A: Physicochem. Eng. Asp. 379 (2011) 36–42.
[11] P. Jarvis, B. Jefferson, J. Gregory, S. Parsons, A review of floc strength and breakage, Water Res. 39 (2005) 3121–3137.
[12] M. Kobayashi, Breakup and strength of polystyrene latex flocs subjected to a converging flow, Colloids Surf. A: Physicochem. Eng. Asp. 235 (2004) 73–78.
[13] F. Xiao, K.M. Lam, X.Y. Li, R.S. Zhong, X.H. Zhang, PIV characterisation of flocculation dynamics and floc structure in water treatment, Colloids Surf. A: Physicochem. Eng. Asp. 379 (2011) 27–35.
[14] E. Barbot, P. Dussouillez, J.Y. Bottero, P. Moulin, Coagulation of bentonite suspension by polyelectrolytes or ferric chloride: Floc breakage and reformation, Chem. Eng. J. 156 (2010) 83–91.
[15] B.B. Mandelbrot, D.E. Passoja, A.J. Paullay, Fractal character of fracture surfaces of metals, Nature 308 (1984) 721–722.
[16] J. Colomer, F. Peters, C. Marrase, Experimental analysis of coagulation of particles under low-shear flow, Water Res. 39 (2005) 2994–3000.
[17] P.T. Spicer, S.E. Pratsinis, Coagulation and framentation: Universal steady-state particle-size distribution, AIChE J. 42 (1996) 1612–1620.
[18] C. Selomulya, R. Amal, G. Bushell, T.D. Waite, Evidence of shear rate dependence on restructuring and breakup of latex aggregates, J. Colloid Interf. Sci. 236 (2001) 67–77.
[19] M.A. Yukselen, J. Gregory, Breakage and re-formation of alum flocs, Environ. Eng. Sci. 19 (2002) 229–236.
[20] J. Duan, J. Gregory, The influence of silicic acid on aluminium hydroxide precipitation and flocculation by aluminium salts, J. Inorg. Biochem. 69 (1998) 193–201.
[21] P.T. Spicer, S.E. Pratsinis, J. Raper, R. Amal, G. Bushell, G. Meesters, Effect of shear schedule on particle size, density, and structure during flocculation in stirred tanks, Powder Technol. 97 (1998) 26–34.
[22] R.K. Chakraborti, J.F. Atkinson, J.E.V. Benschoten, Characterization of alum floc by image analysis, Environ. Sci. Technol. 34 (2000) 3969–3976.
[23] C.P. Johnson, X. Li, B.E. Logan, Settling velocities of fractal aggregates, Environ. Sci. Technol. 30 (1996) 1911–1918.
[24] P. Meakin, Fractal aggregates, Adv. Colloid Interface Sci. 28 (1987) 249–331.
[25] B.E. Logan, J.R. Kilps, Fractal dimensions of aggregates formed in different fluid mechanical environments, Water Res. 29 (1995) 443–453.
[26] P.T. Spicer, S.E. Pratsinis, Shear-induced flocculation: The evolution of floc structure and the shape of the size distribution at steady state, Water Res. 30 (1996) 1049–1056.
[27] D.H. Li, J. Ganczarczyk, Fractal geometry of particle aggregates generated in water and wastewater treatment processes, Environ. Sci. Technol. 23 (1989) 1385–1389.
[28] L.H. Mikkelsen, K. Keiding, The shear sensitivity of activated sludge: An evaluation of the possibility for a standardised floc strength test, Water Res. 36 (2002) 2931–2940.
[29] L.B. Brakalov, A connection between the orthokinetic coagulation capture efficiency of aggregates and their maximum size, Chem. Eng. Sci. 42 (1987) 2373–2383.
[30] R.J. François, Strength of aluminium hydroxide flocs, Water Res. 21 (1987) 1023–1030.
[31] G.C. Bushell, Y.D. Yan, D. Woodfield, J. Raper, R. Amal, On techniques for the measurement of the mass fractal dimension of aggregates, Adv. Colloid Interface Sci. 95 (2002) 1–50.
[32] H. Kockar, M. Bayirli, M. Alper, A new example of the diffusion-limited aggregation: Ni–Cu film patterns, Appl. Surf. Sci. 256 (2010) 2995–2999.
[33] V. Becker, E. Schlauch, M. Behr, H. Briesen, Restructuring of colloidal aggregates in shear flows and limitations of the free-draining approximation, J. Colloid Interf. Sci. 339 (2009) 362–372.
[34] M. Stone, B.G. Krishnappan, Floc morphology and size distributions of cohesive sediment in steady-state flow, Water Res. 37 (2003) 2739–2747.